Available online at www.sciencedirect.com
ScienceDirect
Journal of Luminescence 128 (2008) 661–672
JOURNAL OF LUMINESCENCE
www.elsevier.com/locate/jlumin

Absorption, luminescence, and Raman spectroscopic properties of thin films of benzo-annelated metal-free porphyrazines

Wolfgang Freyer[a,*], Catalin C. Neacsu[a], Markus B. Raschke[b]

[a]*Max-Born-Institut für Nichtlineare Optik und Kurzzeitspektroskopie, Max-Born-Str. 2a, 12489 Berlin, Germany*
[b]*Department of Chemistry, University of Washington, Seattle, Box 351700, WA 98195-1700, USA*

Received 12 February 2007; received in revised form 29 October 2007; accepted 9 November 2007
Available online 19 November 2007

Abstract

Thin film properties of the set of metal-free linearly benzo-annelated porphyrazines, tetra(*tert*-butyl)porphyrazine (*tBu*-$TAPH_2$), tetra(*tert*-butyl)phthalocyanine (*tBu*-PcH_2), tetra(*tert*-butyl)naphthalocyanine (*tBu*-NpH_2), and octaphenyltetraanthraporphyrazine (AnH_2) were studied by laser excitation using micro-Raman and -luminescence spectroscopy. With the exception of *tBu*-$TAPH_2$ all compounds are characterized by a broad absorption pattern mainly due to excitonic coupling. A strong bathochromic energy shift for the Q-band absorption per annelated benzo-moiety was found in solution as well as in the solid state in going from *tBu*-$TAPH_2$ to AnH_2. Films of *tBu*-$TAPH_2$, *tBu*-PcH_2, and *tBu*-NpH_2 exhibit a single broad featureless luminescence band with a large Stokes shift, which originates from an excitonic state. In addition, *tBu*-$TAPH_2$ and *tBu*-NpH_2 exhibit photoluminescence peaks emerging from monomer-like molecules. These porphyrazines are the only ones known to show two luminescence peaks each. A systematic decrease in luminescence efficiency of thin films is observed and can be attributed to exciton coupling and migration leading to efficient quenching of the radiative decay channels. It also allows for Raman spectroscopic characterization of the thin films and for the case of *tBu*-NpH_2 in highly concentrated solutions.The different resonance Raman spectra of the compounds can be used as fingerprint for distinguishing the degree of benzo-annelation.

Keywords: Porphyrazines; Phthalocyanines; Naphthalocyanines; Anthralocyanines; Thin film; Absorption; Photoluminescence; Micro-Raman; Excitonic coupling

1. Introduction

Phthalocyanine derivatives are of increasing technological relevance due to their unique photophysical properties. These compounds have proven great potential as materials for optoelectric and electronic devices for solar cells [1–3], organic light-emitting diodes (OLED) [4,5], semiconductor layers [6,7], or optical limiters [8,9]. For most of these device applications, which largely rely on the electronic excited state properties, phthalocyanines are involved in the form of solid-layered structures or thin films. This makes a detailed understanding of the thin film properties highly desirable. Most studies so far have addressed the structural aspects of the molecular arrangement of phthalocyanines in the condensed thin film phase using UPS, XPS or NEXAFS [10–13]. Valuable additional information in particular concerning the optical properties can be gained from luminescence spectroscopy. This, however, is challenging due to the low fluorescence quantum yield in dilute solution [14], which is expected to be further reduced down to 10^{-5} in thin films due to strong intermolecular coupling [15]. The luminescence studies of solid metal-free porphyrazines have been limited to *unsubstituted* metal-free phthalocyanine PcH_2 in the form of thin films [16–20], crystals [21], liquid crystals [22,23], as well as to some of their metal complexes [16,21] using laser excitation. Moreover, few studies have yet addressed the Raman spectra of the metal-free porphyrazines, with only PcH_2 [18,24] and NpH_2 [25] having been studied.

*Corresponding author. Tel.: +49 30 6392 1343; fax: +49 30 6392 1309.
E-mail address: freyer@mbi-berlin.de (W. Freyer).

0022-2313/$ - see front matter © 2007 Elsevier B.V. All rights reserved.
doi:10.1016/j.jlumin.2007.11.070

Though porphyrazines bearing a different number of fused benzo-moieties are spectroscopically well investigated in solution [14,26], a complete spectroscopic characterization of their film properties is not available. To learn more about the influence of the so-called benzo-annelation which results in an extension of the π-system, we systematically investigated the spectroscopic response of thin films of a set of benzo-annelated metal-free porphyrazines: tetra (*tert*-butyl)porphyrazine (*tBu*-$TAPH_2$), tetra(*tert*-butyl) phthalocyanine(*tBu*-PcH_2), tetra(*tert*-butyl)naphthalocyanine (*tBu*-NpH_2), and octaphenyltetraanthra porphyrazine (AnH_2) (see Fig. 1) by laser excitation at 543, 633, and 806 nm. Here we monitored their luminescence and/or Raman spectra by employing a micro-fluorescence and -Raman spectroscopic approach. This method allows the study of smallest sample volumes. We also refer to investigations of unsubstituted derivatives PcH_2 and NpH_2. Since the centres of the porphyrazine ligands are not coordinated with any central metal ion, the electronic states are exclusively of porphyrazine ligand origin. As a consequence the monomers of these compounds have a higher fluorescence quantum yield (0.01–0.4) than their metal-centred compounds [14]. This issue is important because the luminescence quantum yield in the solid state can be lowered by some orders of magnitude by excitonic coupling [16].

The strong fluorescence quenching allows for the simultaneous observation of the characteristic Raman response of the respective thin film constituents. A comparison of luminescence and Raman emission in going from solution to the solid state allows drawing some conclusions on relaxation behaviour and its dependence on the degree of benzo-annelation.

In addition, to mimic strong interaction between porphyrazine molecules, we investigated dimers/aggregates of the compounds in solution as precursors of the solid state. Here, samples of variable concentrations were investigated.

2. Experimental

The synthesis and purification of the four compounds chosen for our investigation was described previously [14]. The monomers of *tBu*-$TAPH_2$, *tBu*-PcH_2, and *tBu*-NpH_2

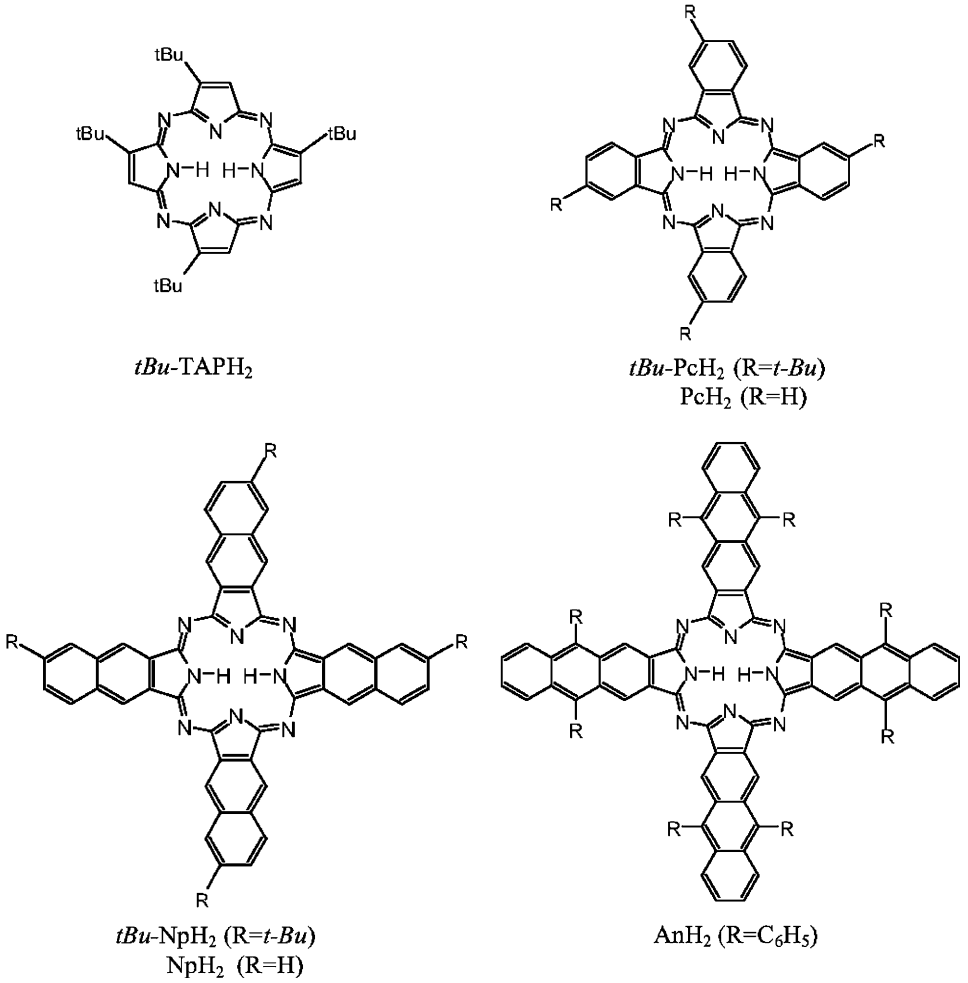

tBu-$TAPH_2$

tBu-PcH_2 (R=*t-Bu*)
PcH_2 (R=H)

tBu-NpH_2 (R=*t-Bu*)
NpH_2 (R=H)

AnH_2 (R=C_6H_5)

Fig. 1. Structure formulae of linearly annelated porphyrazines: tetra(*tert*-butyl) porphyrazine (*tBu*-$TAPH_2$), tetra(*tert*-butyl)phthalocyanine (*tBu*-PcH_2), phthalocyanine (PcH_2), tetra(*tert*-butyl)naphthalocyanine (*tBu*-NpH_2), tetranaphthoporphyrazine (NpH_2), and octaphenyltetraanthraporphyrazine (AnH_2).

exist as a mixture of several (due to the different positions of the *tert*-butyl groups) isomers, which are formed statistically during the synthesis. For steric reasons some isomers are preferred in the mixture. Separation of these various isomers by chromatography is extremely difficult, yielding fractions containing a mixture of at least two isomers which exhibit nearly identical electronic absorption and emission spectra [14]. Therefore, absorption and emission spectra are for a representative mixture of all isomers.

Thin films of *tBu*-TAPH_2, *tBu*-PcH_2, and *tBu*-NpH_2 were prepared by sublimation deposition onto quartz cover slides under high vacuum conditions (base pressure $<1.3\times10^{-6}$ mbar). The quartz slides were cleaned in H_2SO_4:H_2O_2:H_2O (1:1:3), rinsed with deionized water (Millipore), and dry blown in an argon stream. The evaporator was positioned 5 cm from the substrate surface. The sublimation temperatures of *tBu*-TAPH_2, *tBu*-PcH_2, and *tBu*-NpH_2 are 170, 260, and 500 °C, respectively. To ensure that thermal degradation can be precluded, the deposited films were dissolved in dioxane and analysed by UV–vis spectroscopy. Typical film thicknesses in the range of 10–400 nm were used as estimated by a quartz crystal microbalance and atomic force microscopy (AFM) using scratch testing (Nano Scope III, Digital Instruments). Since AnH_2 is not stable during sublimation, AnH_2 films were prepared by spin coating from $\sim5\times10^{-4}$ to 10^{-5} M benzene solutions on quartz slides. For the AnH_2 samples investigated the thickness was estimated to be of order ~80 and ~140 nm, respectively, via UV–vis absorption measurements. Furthermore, we compared *tBu*-PcH_2 films of different thickness produced by vacuum deposition and by spin coating and found to exhibit the absorption spectrum of the α-polymorph for all films. To obtain information about the quality of the films we investigated the surface morphology by AFM. Since the films were not annealed after sublimation, formation of the α-phase is assumed [27]. The AFM analysis of the sublimed films of *tBu*-TAPH_2 and *tBu*-PcH_2 shows smooth surfaces. The image of a *tBu*-PcH_2 film is identical to that of an α-phase for Pc-H_2 [18,28–30]. The AFM images for the different *tBu*-NpH_2 films display a homogeneous distribution of small spherical protrusions of similar size and shape (data not shown). Absorption measurements were carried out using a UV/vis/NIR spectrometer (Lambda 900/Perkin–Elmer). Fluorescence spectra of highly diluted solutions (absorption at the excitation wavelength = 0.005–0.02) were recorded with a spectrofluorometer (Fluorolog 2, SPEX industries) using a standard quartz cell (d = 10 mm). Fluorescence light was collected in the right angle configuration with respect to the excitation. The bandpass of both excitation and emission was 0.6 nm. The solvents used were of spectrograde quality (UVASOL) from Merck.

For the laser-induced fluorescence measurements a micro-Raman spectroscopy setup was employed. It consists of a confocal microscope (objective: NA = 0.80, WD = 0.68 mm) used in epi-illumination and -detection configuration. The Raman and fluorescence light was collected in the backscattered direction, spectrally selected using dichroic filters and an imaging spectrograph, and detected with a liquid-nitrogen-cooled back-illuminated charged coupled device (CCD, Roper Scientific). The detector is sensitive up to a wavelength of 1100 nm. Laser excitation wavelengths of 543, 633, and 806 nm were employed as provided from HeNe and Ti:Sapphire laser sources. The laser fluence was set to 40–90 kW cm^{-2}. For the laser-induced fluorescence measurements of solutions standard quartz cells (d = 1 and 10 mm) were used. Here, for the fluorescence measurements the laser excitation volume was positioned directly behind the entrance cell wall to avoid re-absorption processes.

3. Results and discussion

3.1. Absorption spectra of porphyrazines in solution

The absorption spectra of *tBu*-TAPH_2 (λ_{max}: 623 and 522 nm), *tBu*-PcH_2 (λ_{max}: 700 and 661 nm), *tBu*-NpH_2 (λ_{max}: 785 and 771 nm (sh)) and AnH_2 (λ_{max}: 904 and 884 nm) in CCl_4 are displayed in Fig. 2. They show a red shift of the main Q-band absorption maxima together with their vibrational structure of about 100 nm per annelated benzo moiety. The peak positions for the different components are also summarized in Table 1. This bathochromic shift due to the extension of the π-system of the macrocycle is in accordance with investigations of other benzo-annelated porphyrazines [14,31,32]. All compounds exhibit a splitting of the Q band into a Q_x and a Q_y part. With increasing benzo-annelation the energy difference between both transitions decreases (*tBu*-TAPH_2 ($\Delta\sim3110$ cm^{-1}); *tBu*-PcH_2 ($\Delta\sim840$ cm^{-1}); *tBu*-NpH_2 ($\Delta\sim230$ cm^{-1}); AnH_2 ($\Delta\sim250$ cm^{-1}). This splitting is also observed for *tBu*-NpH_2 in CCl_4 for concentrations down to 10^{-8} mol l^{-1}, albeit with only $\Delta\sim230$ cm^{-1} it is comparatively weak. The splitting for *tBu*-NpH_2 could not be resolved in benzene [14].

In Fig. 3, the absorption spectrum of a highly concentrated *tBu*-NpH_2 solution ($\sim1.9\times10^{-2}$ M in CCl_4) is shown with λ_{max}: 693 nm and a shoulder at λ_{max}: 760 nm. This pronounced blue shift of the broad absorption can be attributed to aggregate formation. We estimate that more than about 95% of *tBu*-NpH_2 molecules have formed aggregates at the given concentration. The assignment of the aggregate formation as deduced from our fluorescence analysis will be discussed below. The broadness of the absorption profile may reflect the existence of numerous conformers in solution. In contrast to *tBu*-NpH_2, *tBu*-TAPH_2 does not show any aggregation in CCl_4 even at concentrations as high as 10^{-2} M. In comparison, the tendency for aggregate formation for *tBu*-PcH_2 in CCl_4 is qualitatively found to be intermediate (data not shown).

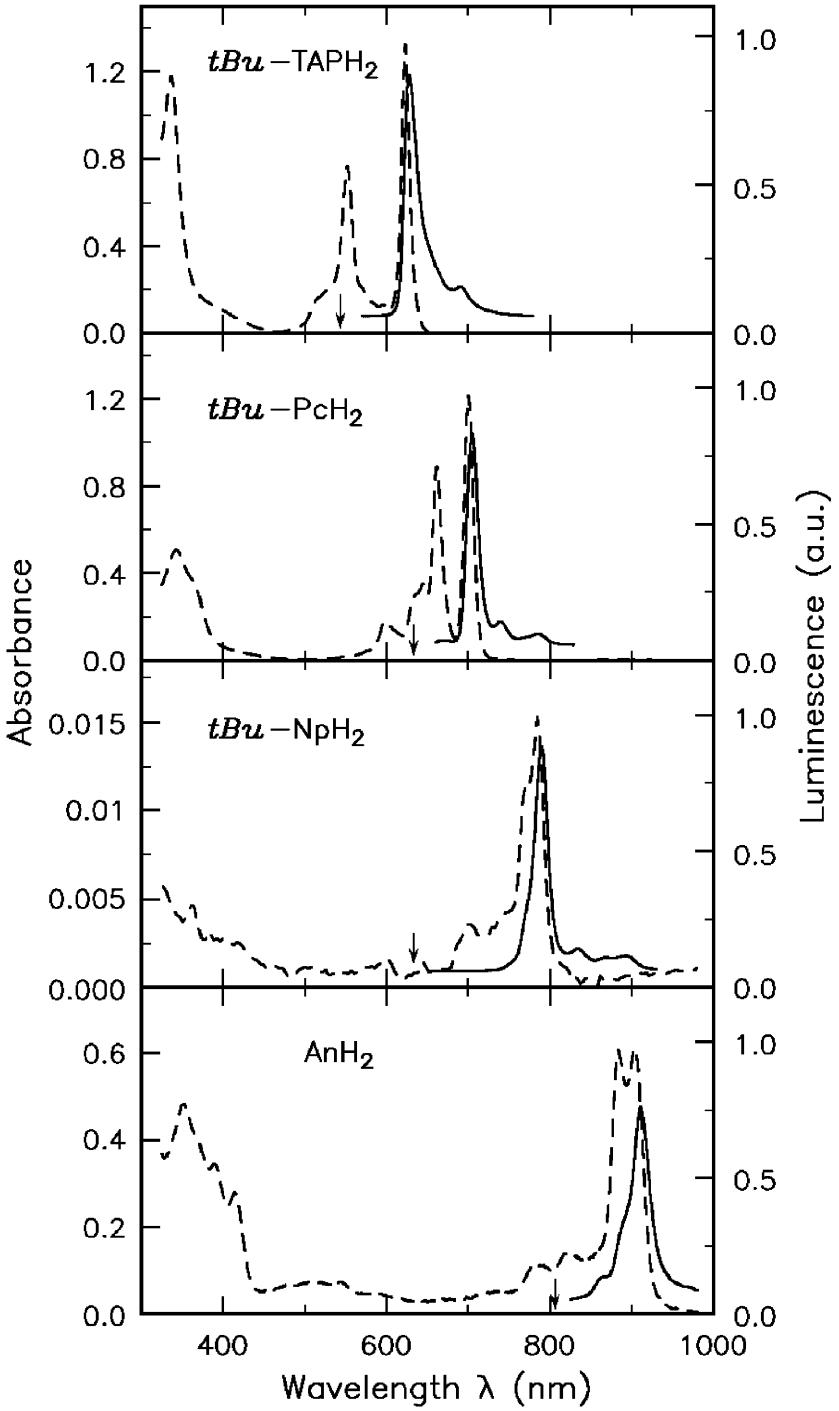

Fig. 2. Absorption (dashed lines) and fluorescence spectra (solid lines) of porphyrazines dissolved in CCl_4, indicating a systematic shift of the Q-band region with increasing benzo-annelation. Small arrows represent the laser excitation wavelengths. *tBu*-$TAPH_2$: $c = 1.56 \times 10^{-5}$ M; *tBu*-PcH_2: $c = 6.4 \times 10^{-6}$ M; *tBu*-NpH_2: $c = 4.2 \times 10^{-8}$ M; AnH_2: $c = 8 \times 10^{-6}$ M.

3.2. Absorption spectra of porphyrazines in the solid state

Corresponding absorption spectra of thin films of the four different linearly benzo-annelated porphyrazines are presented in Fig. 4. The absorption bands of the Q-band region in the solid-state spectra are shifted and broadened to longer wavelengths in the series of *tBu*-TAP-H_2 (628, 556 nm), *tBu*-Pc-H_2 (692 nm (sh), 613 nm), *tBu*Np-H_2 (797, 718 nm), and An-H_2 (915 nm (sh), 904 nm) relative to their absorption spectra in solution. In addition, the intensity of the B-band region (around 330 nm) is strongly increased. In Figs. 3 and 4, a number of differences between solid state and solution spectra can be seen:

First, the absorption spectrum of *tBu*-TAP-H_2 in the solid state (λ_{max}: 628, 556 nm) resembles that in CCl_4 solution (λ_{max}: 623, 522 nm). Q-band splitting can unambiguously

Table 1
Absorption and luminescence characteristics of metal-free porphyrazines in CCl_4 (s) and thin films (f)

Compounds		λ_{abs}^{max} (nm)		ΔQ (cm^{-1})	λ_{lum}^{max} (nm)	Stokes shift (cm^{-1})
		Q_x	Q_y			
tBu-$TAPH_2$	s	623	522	3110	628	127
tBu-$TAPH_2$	f	628	556	2060	628 and 695	1550 and 0[a]
tBu-PcH_2	s	700	661	840	705	100
PcH_2[b]	s	693	656	800	698	110
tBu-PcH_2	f	692 sh	613	1860	862	2900
PcH_2[c]	f	690 sh	630			
β-PcH_2[d]	f	712	651	1300		
tBu-NpH_2	s	785	771	230	790	80
tBu-NpH_2	s[e]	760 sh	693	1270	790[f]	
tBu-NpH_2	f[g]	798	(–)		(–)[h]	
tBu-NpH_2	f[i]	797; 718	(–)		(882 and 815)[j]	(1200 and 300)[j]
AnH_2	s	904	884	250	910	70
AnH_2	f[k]	915	904 sh	160	(–)[h]	
AnH_2	f[l]	958	917 sh	470	(–)[h]	

[a]Resonance luminescence, see discussion.
[b]Benzene [14].
[c]Ref. [18].
[d]Refs. [18,33].
[e]1.86×10^{-2} M in CCl_4.
[f]Monomer fluorescence.
[g]20 nm film.
[h]Not observed.
[i]60 nm film.
[j]See discussion.
[k]80 nm film.
[l]140 nm film.

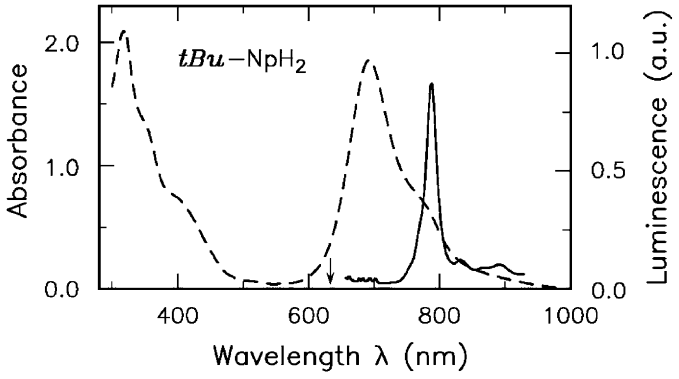

Fig. 3. Electronic absorption (dashed line) and fluorescence spectrum (solid line, λ_{exc}: 633 nm) of a highly concentrated CCl_4 solution of *tBu*-NpH_2 ($c = 1.86 \times 10^{-2}$ M). The aggregation effect manifests itself in the pronounced blue shift of the absorption peak. The fluorescence at 790 nm is due to fluorescence of the monomer. Raman scattering can be seen in the range 650–700 nm (see also Fig. 6).

be identified for *tBu*-TAP-H_2 ($\Delta \sim 2060\ cm^{-1}$) only. The corresponding value is lower than that in solution. The Q_y transition shifts more than the Q_x one, but both show a bathochromic shift. Moreover, it is evident that the intensity of the shoulder at ~530 nm is increased at film thicknesses higher than 100 nm while in the range 20–100 nm is not. The full-width at half-maximum (FWHM) of the Q_y and Q_x transitions, both in solution and film, are approximately the same. Note that the long-wavelength absorption edge is identical with that in solution, e.g., a near-IR absorption tail does not exist. Interestingly, the positions of the Q-band maxima shift with increasing film thickness (20–500 nm) at 2 nm only.

Second, the absorption profile of *tBu*-$TAPH_2$ differs significantly compared to those of *tBu*-PcH_2, *tBu*-NpH_2, and AnH_2, where major broadenings, peak shifts, and pronounced long-wavelength tails are evident in the case of thin films compared to solution.

For *tBu*-PcH_2 a blue-shifted broad absorption with λ_{max}: 613 nm with a shoulder at 692 nm is observed, which resembles the spectra for α-PcH_2 (630 nm with a shoulder at 690 nm) [18,19], while the *β*-form would exhibit two bands of similar intensity at 712 and 651 nm ($\Delta \sim 1300\ cm^{-1}$) [33]. Although a second absorption maximum of *tBu*-PcH_2 is not resolved in the α-phase, band analysis gives $\Delta \sim 1860\ cm^{-1}$ between the main maximum and the shoulder. The value of $\Delta \sim 1860\ cm^{-1}$ is much larger in the solid state than in solution and is in contrast to the situation of *tBu*-$TAPH_2$. As for *tBu*-$TAPH_2$, the absorption spectra of all *tBu*-PcH_2 films with different thicknesses (6–450 nm) exhibit a similar spectral shape and the absorption maxima differ by 2 nm only. Therefore, only one absorption spectrum of a 430 nm film is shown in Fig. 4.

Third, the absorption of a thin *tBu*-NpH_2 film of only 20 nm thickness (Fig. 4, dotted line) resembles the spectral

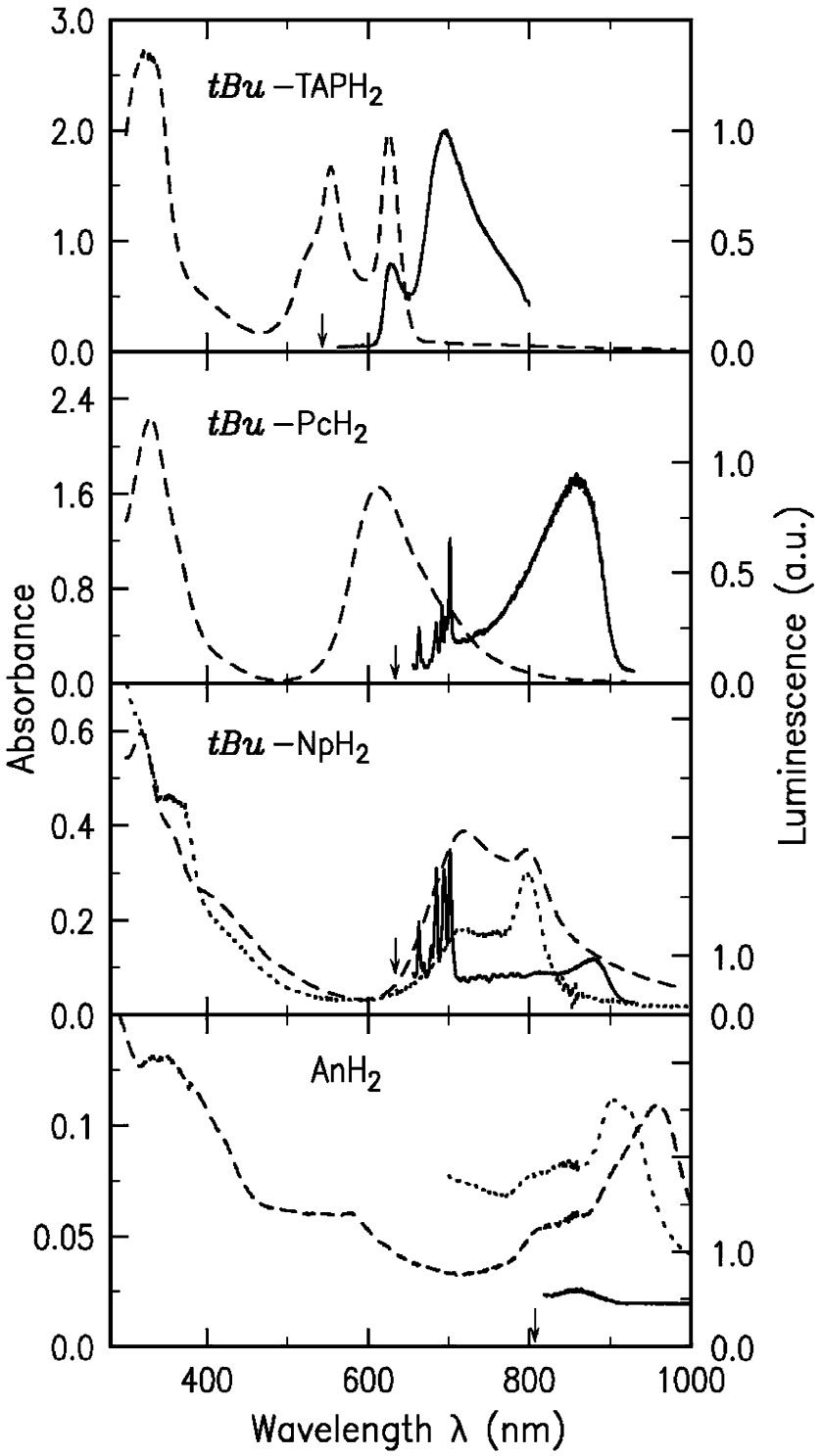

Fig. 4. Electronic absorption (dashed lines) and luminescence spectra (solid lines) of thin films of different thicknesses of porphyrazines deposited onto quartz plates. Vertical arrows indicate the laser excitation wavelengths. Due to the strong luminescence quenching, Raman emission is observed. *tBu*-$TAPH_2$ (d~350 nm), *tBu*-PcH_2 (d~430 nm), *tBu*-NpH_2 (d~20 nm, dotted line; d~60 nm, dashed line); and AnH_2 (d~80 nm, dotted line; d~140 nm, dashed line).

characteristic of the dilute solution in CCl_4, with the response being dominated by the 798 nm band. However, this band is red-shifted by 12 nm in comparison to the spectrum recorded in CCl_4. In addition, a weakly broadened absorption is observed at 718 nm.

In the absorption spectra of a 60 nm film of *tBu*-NpH_2 this unsymmetrically broad blue-shifted absorption peak with λ_{max}: 718 nm dominates the spectrum. A second maximum is at λ_{max}: 797 nm (Fig. 4, dashed line), which is identical to that for the 20 nm film. The spectrum of the

60 nm film possesses a weak but broad tail to the red. The response for the blue-shifted component (718 nm) is similar to the dominant features observed in concentrated solution with $\lambda_{max} = 693$ nm (shoulder at λ_{max}: 760 nm; $\Delta \sim 1270\,cm^{-1}$).

Fourth, a similar but inverse behaviour is found for AnH_2 films. Here the absorption behaviour (film thickness 80 nm, dotted line in Fig. 4) is characterized by a non-symmetric broad absorption band with λ_{max} at 904 nm and a shoulder at 915 nm ($\Delta \sim 160\,cm^{-1}$). For thicker films (140 nm, dashed line) the absorption maximum shifts to longer wavelength (λ_{max}: 958 nm) relative to the solution spectrum and has a non-symmetric absorption profile (band analysis gives ~917 nm for the short-wavelength shoulder) ($\Delta \sim 470\,cm^{-1}$).

3.3. Discussion of the absorption spectra of porphyrazines

To interpret these experimental results, Fig. 5 can be consulted. In metal-free porphyrazines band splitting in solution into a Q_x and a Q_y band (see Fig. 5A) is due to molecular symmetry properties [34]. It is attributed to the reduction of D_{4h} symmetry to D_{2h} or lower (with Δ then being a measure for the departure from D_{4h} symmetry). Therefore, metal phthalocyanines with D_{4h} symmetry only show a single intense Q-band absorption due to the degenerated excited state. From the very small splitting observed for *tBu*-NpH_2 and AnH_2 one can conclude that the symmetry for these porphyrazines is close to D_{4h}.

The absorption spectra of the films show a more complex behaviour. The exciton model developed by Davydov [36] and Kasha [35] and superimposed by molecular distortion [33,37,38] has been successfully applied to PcH_2-films [33,39–41] to explain the absorption spectrum. However, this model does not consider any interaction between non-neighbour units. These interactions could be significant in porphyrazine films.

In the films of the different porphyrazines significant changes of the peak wavelengths and intensities are observed, partly affected by the film thickness. In the case of a strong excitonic coupling one would expect the absorption to be either strong blue-shifted relative to the monomer (transition to b_2), or red-shifted with excitation into the lowest exciton allowed b and b_1 and occupation of the upper exciton forbidden band b_2 (see Fig. 5B). Both possibilities have been found in dependence of the benzo-annellation degree. Which excitonic states are allowed or forbidden depends on the alignment of the molecules in the film, specifically the angle θ between the line connecting the porphyrazine centre and the porphyrazine molecular planes, the molecular symmetry properties, and consequently on the orientation of the transition dipoles. For example, in contrast to the higher benzo-annelated porphyrazines, the pattern of solid state and solution spectra for *tBu*-$TAPH_2$ are very similar, differing only in the position of the Q_y band and its shoulder at ~530 nm with increased intensity. We conclude that the porphyrazine core with its bulky *tert*-butyl groups seems to hinder efficient excitonic coupling within a pile in the film. This is also supported by the observation that *tBu*-$TAPH_2$ in non-polar solvents like CCl_4 does not show any aggregation even at high concentrations. Moreover, the Q-band position for films with different thicknesses is almost at the same wavelength compared to solution, backing also the assumption that there is no strong interaction between substrate surface and *tBu*-$TAPH_2$. On the other hand, the increased intensity of the B-band region together with emerging of the shoulder at 530 nm with increasing film thickness reveal a certain degree of excitonic coupling. In contrast, the absorption spectra of *tBu*-PcH_2 imply a strong coupling behaviour with the transition into the lowest excitonic band b_1 being forbidden and the transition into the upper excitonic band b_2 being allowed (Fig. 5B). The similarity between the absorption spectra of *tBu*-PcH_2 and PcH_2 [18] implies that the bulky *tert*-butyl substituents in the *tBu*-PcH_2 isomers seem not to influence the structure within the film significantly. However, in the case of the large π-systems of *tBu*-NpH_2 and AnH_2 films their

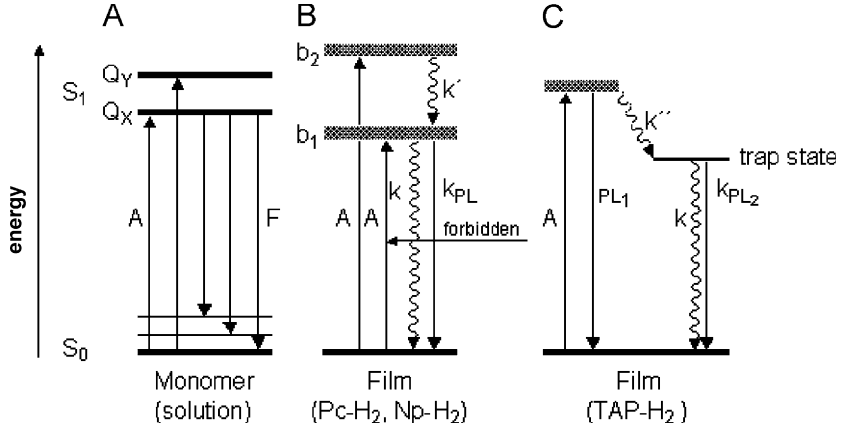

Fig. 5. Simplified energy level schemes for the excitation and deactivation processes of porphyrazines in solution (A) and in the solid state (B, C). A: transitions to Q_x and Q_y levels of monomers with D_{2h} symmetry. The horizontal bars in B and C represent the exciton bands. Solid arrows: absorption and luminescence transitions. Wiggled arrows: radiationless processes, PL: photoluminescence.

thickness influences both the absorption pattern and the position of the maxima. These effects may reflect the existence of two species exhibiting different excitonic interaction which results in populations of two different excitonic states. We attribute the absorption peak at 797 nm in the 20 nm film for *tBu*-NpH_2 to the population of the exciton band b_1, while in the thicker film population of the b_2 band seems to dominate. In contrast, for AnH_2, with increasing film thickness two absorption patterns of bathochromic-shifted peaks were distinguished relative to the peak of the monomer in solution which may interpreted as population of two different excitonic states of type b_1. These effects may reflect a change in the organization of the porphyrazine molecules in the film caused for example by changes of the molecular packing or the orientation in going from thinner to thicker films for *tBu*-NpH_2 and AnH_2. This interpretation is also supported by investigations on unsubstituted metallo naphthalocyanines, where the first deposited molecules show a different alignment compared to subsequently added layers. This leads to films where the molecules are in the face-to-face or eclipsed, slipped mode [42] (unfortunately, absorption spectra are not given). Moreover, it is known that thin films of some metallo-phthalocyanines exhibit a certain degree of molecular ordering, with the degree of the preferential orientation decreasing with increasing film thickness [43,44]. Recently the existence of two polymorphic forms during the annealing process of a PcH_2 film [45] and the dependence of the visible/NIR spectra of the film morphology of chloroaluminium phthalocyanine [7] have also been shown by absorption spectroscopy. It seems that, in contrast to the *tBu*-PcH_2 film, the bulky *tert*-butyl groups in the larger π-systems of *tBu*-NpH_2 and AnH_2 gain more influence and could be responsible for a different geometrical orientation of the molecules depending on the thickness of the film.

3.4. Luminescence spectra

A conventional fluorescence spectrometer using Xenon lamp excitation gives exact fluorescence maxima under right angle configuration *only* when the fluorescence measurement is carried out for highly diluted samples ($<10^{-7}$ M). The main reason is the strong re-absorption process at higher concentrations that leads, e.g., to an apparent red shift of the fluorescence maxima for some phthalocyanines [46]. In our experimental approach the re-absorption of emitted radiation is suppressed since the luminescence light from the sample volume is directly emitted just several microns behind the cuvette wall. This allows for accurate and highly sensitive measurements of solutions at higher ($>10^{-5}$ M) concentrations. We have assessed the applicability of our method comparing the luminescence spectra of different porphyrazines at low concentrations with that using a conventional fluorescence spectrometer. In addition, by varying the concentration we did not find changes in the position of the fluorescence maxima measured with our method.

The fluorescence spectra of *tBu*-$TAPH_2$ (maxima are given in brackets; see also Table 1) (λ_{fl}: 628 nm), *tBu*-PcH_2 (λ_{fl}: 705 nm), *tBu*-NpH_2 (λ_{fl}: 790 nm), and AnH_2 (λ_{fl}: 910 nm) dissolved in CCl_4 are shown in Fig. 2 (solid lines). As expected, the Stokes shift of the compounds is small (a few nm) [14] and gives rise to a large overlap of the absorption and emission spectra. All fluorescence spectra exhibit vibrational structure. The aggregates of *tBu*-NpH_2 do not fluoresce and the fluorescence that can be seen in Fig. 3 results from the few percent of monomers present at equilibrium. The same behaviour is found for *tBu*-PcH_2.

The absence of aggregate fluorescence for *tBu*-NpH_2 and *tBu*-PcH_2 is consistent with the recent interpretation for the case of substituted metallo-phthalocyanine dimers/aggregates [46,47] or even tetramers [48].[1]

We find that the already low quantum efficiency for the monomers of *tBu*-PcH_2 and *tBu*-NpH_2 in solution (Φ_f: 0.43, 0.19) [14] is greatly reduced due to strong intermolecular interaction in highly concentrated solutions. This is in agreement with investigations of other phthalocyanines where this strong quenching is attributed to efficient pathways for energy transfer and redistribution [51].

In Fig. 4, the luminescence from films of *tBu*-$TAPH_2$, *tBu*-PcH_2, *tBu*-NpH_2, and AnH_2 at room temperature is shown. The spectral characteristics of the emission (Table 1) are very different depending on the number of benzo-moieties attached to the core porphyrazine.

An-H_2 films do not show any luminescence in the range >900 nm irrespective of the excitation wavelengths used (λ_{exc}: 543, 633, 806 nm).[2] Note that with $\Phi_{fl} = 0.01$ the fluorescence quantum yield of An-H_2 in solution is already very low [14].

In contrast to the porphyrazines dissolved in CCl_4, the luminescence of films of *tBu*-$TAPH_2$ (λ_{lum}: 628, 695 nm; λ_{exc}: 543 nm;), *tBu*-PcH_2 (λ_{lum}: 862 nm, λ_{exc}: 633 nm), and *tBu*-NpH_2 (λ_{lum}: 882 nm and very weak at 815 nm, λ_{exc}: 633 nm) show unusually broad but distinct emission bands centred at the given maxima with extremely low intensity. For the PcH_2 film a quantum yield of $\Phi = 10^{-4}$ was estimated [16]. The relative intensity decreases significantly in going from *tBu*-$TAPH_2$ to *tBu*-NpH_2. The Stokes shift of the long-wavelength luminescence for *tBu*-$TAPH_2$ ($\Delta\sim1550\,cm^{-1}$), *tBu*-PcH_2 ($\Delta\sim2900\,cm^{-1}$; related to the shoulder in the absorption spectrum at 692 nm), and *tBu*-NpH_2 ($\Delta\sim1200\,cm^{-1}$; related to the superimposed absorption maximum at 797 nm) is unusually large with a small overlap between the long-wavelength absorption tail and the emission spectrum. It is noteworthy that in the case of

[1] An exception is a very weak yet strongly red-shifted fluorescence reported for the μ-oxo dimer of silicon phthalocyanine in solution [49,50].

[2] No reproducible luminescence signature could be obtained, possibly due to degradation of AnH_2 under the excitation conditions. This degradation process is particularly evident for laser excitation at $\lambda_{exc} = 355$ nm.

*t*Bu-TAPH$_2$ excited with λ_{exc}: 543 nm the photoluminescence still exhibits a small resonance signal centred at λ_{lum}: 628 nm in addition to the strong Stokes-shifted emission centred at λ_{lum}: 695 nm. For λ_{exc}: 633 nm the position of the emission maximum at λ_{lum}: 695 nm remains unchanged. Furthermore, also the 60 nm film of *t*Bu-NpH$_2$ indicates a very weak luminescence at 815 nm (Stokes shift $\Delta \sim 300\,cm^{-1}$). Unfortunately, the thinner 20 nm film did not show any luminescence signal. Both *t*Bu-TAPH$_2$ and *t*Bu-NpH$_2$ are the first porphyrazines found to exhibit two luminescence signatures in the solid state, with one of them being resonance luminescence.

3.5. Discussion of luminescence spectra

For a consistent interpretation of the absorption and luminescence behaviour observed in the set of porphyrazines investigated we propose the following model as depicted in Fig. 5. Here, illustration 5A explains the fluorescence of the porphyrazines from S_1 in solution with a small Stokes shift and a vibrational structure of the fluorescence.

The luminescence behaviour of films (Fig. 5B) differs from that in solution. After excitation of the metal-free porphyrazines in the films, excitonic states are populated depending on the relative molecular orientation and intermolecular coupling. The deactivation of the excited excitonic state can occur via radiative or non-radiative decay. Given the low quantum efficiency our results indicate that non-radiative relaxation processes of excited excitonic states are dominant in the solid films (e.g. internal conversion, exciton–exciton annihilation, formation of triplet excitons, and impurity traps). The radiative site in the films can be attributed to low-lying localized excitons, surface excitons, impurities, and structural changes within or between molecules. From our experimental findings the following conclusions can be drawn:

First: The luminescence behaviour of *t*Bu-TAPH$_2$ films with the appearance of two pronounced luminescence bands with maxima at λ_{lum}: 695 nm and λ_{lum}: 628 nm is unusual. This indicates that two different kinds of states exist affecting the decay process. The Stokes shift of $\sim 1550\,cm^{-1}$ nm for the luminescence peak at 695 nm is lower than that observed for *t*Bu-PcH$_2$ ($\sim 2900\,cm^{-1}$), while the photoluminescence at 628 nm represents a resonance luminescence. According to our measured absorption spectra of the films, the intermolecular interaction between *t*Bu-TAPH$_2$ molecules should be weak and the large splitting effect is mainly due to the molecular symmetry properties and not due to the excitonic coupling. We interpret the resonance luminescence to be the free exciton luminescence (Frenkel excitons). The *t*Bu-TAPH$_2$ molecules seem to couple neither in the films (100–500 nm thickness) nor in solution even at high concentrations due to their bulky *tert*-butyl groups. Thus, it might be presumed that the 628 nm luminescence in the film originates from monomer-like molecules due to lattice distortion occurring at the crystal surface. This implies an allowed transition into the lowest excited exciton band from which luminescence is allowed (PL_1 in Fig. 5C). Similar effects were observed in pyren [52] or a perylene derivative [53]. Furthermore, the influence of bulky alkyl-substituents investigated on specially substituted perylene [54] and bifluorene [55] derivatives exhibits only a small Stokes shift, while the expected long-wavelength luminescence was suppressed due to the presence of alkyl chains.

On the other hand, the broad red-shifted and structureless luminescence at 695 nm is far away from the long-wavelength absorption edge. This luminescence (denoted as PL_2 in Fig. 5C) might emerge from a trapping state immediately after creation, with participation of some states formed at a lattice site of neighbouring molecules in a stack. Because the *tert*-butyl substituents give rise to the existence of several geometrically distinct isomers it does not seem unreasonable to assume stacks with different orientation within the same film which can act as trap for excitons compared to the undisturbed *t*Bu-TAPH$_2$ molecules. On the other hand, impurities and defects which can also trap excitons must be taken into consideration. An additional explanation involves a certain number of molecules which give rise to the emergence of the broad shoulder at $\sim$530 nm in films with thicknesses >100 nm. This fact, an increased intensity of the B-band region and the low luminescence intensity implies a strong excitonic coupling with population of the exciton band b_2 in Fig. 5B. Deactivation of this state and luminescence from a lower lying state would then explain the large Stokes shift (see also the following part).

Second: In case of a strong excitonic coupling with a strong blue-shifted absorption relative to the monomer as found for *t*Bu-Pc-H$_2$ and for the thicker film of *t*Bu-NpH$_2$, only the higher excitonic transition to b_2 is allowed (Fig. 5B). The broad absorption and luminescence envelopes, and the large Stokes shift together with the absence of any discernible vibrational substructure in the emission band from *t*Bu-PcH$_2$ and *t*Bu-NpH$_2$ films suggest that the molecules in the film couple stronger in the excited state than in the ground state. The large Stokes shift for *t*Bu-PcH$_2$ ($\sim 2900\,cm^{-1}$) and for *t*Bu-NpH$_2$ ($\sim 1200\,cm^{-1}$) could be associated with a change in the molecular conformation in the solid state. Other examples for the appearance of a broad structureless emission have been observed in films of aromatic compounds like perylene and their derivatives [56–58], pyrene [52,59], chrysene and anthracene [59], 1,2-diarylethene derivatives [60], polymer films containing aromatic derivatives covalently bound [61–63], as well as the already mentioned phthalocyanines [16–21]. Most of these results have been interpreted as excimer luminescence.

According to Fig. 5B, the allowed higher energetic excitonic state b_2 of *t*Bu-PcH$_2$ and *t*Bu-NpH$_2$ can deactivate radiationless via the lower excitonic state b_1 with the corresponding rate constants k' and k. If k is faster than the rate k_{PL} for the radiative decay of this state no

photoluminescence PL is observed. The absence of any luminescence of dimers/aggregates of *tBu*-PcH_2 and *tBu*-NpH_2 in solution might exclusively result from non-radiative deactivation processes of both excitonic states with very fast k and k'. However, in the solid state photoluminescence is observed. That means k_{PL} is at least of the same order of magnitude or larger compared to k. Only in that case a very weak luminescence with a large Stokes shift can be detected. A reason why photoemission from a forbidden state is observed seems to be closely connected with the pronounced broad and weak tail to the red in the absorption spectra of the films (Fig. 4). A possible explanation could be the contributions to vibronic levels of the ground state, which could be weakly allowed. This was very recently suggested to interpret the dimer fluorescence in solution of a μ-oxy silicon phthalocyanine [49]. On the other hand, Orti et al. [64] calculated two allowed transitions for the NIR region of a Pc-H_2 dimer. Both calculated transitions at 827 and 742 nm exhibit low oscillator strength and fall into the range of the weak wings in the *tBu*-PcH_2 film.

Similar to the case of the *tBu*-$TAPH_2$ films two luminescence signals of *tBu*-NpH_2 were also observed in the film. We interpret the very weak luminescence of *tBu*-NpH_2 at 815 nm to originate from the 797 nm peak in the absorption spectrum of the 60 nm film. In this case the Stokes shift is 300 cm^{-1} only. The magnitude is similar to that found in solution (80 cm^{-1}). Consequently, the emission at 815 nm seems to caused by a monomer-like structure in the film. Both emissions found in the Np-H_2 film (and in the *tBu*-$TAPH_2$ film, too) could arise from molecules existing in a different molecular arrangement for example by occurrence of different staggered components due to the presence of *tert*-butyl groups which could influence the order of the films.

3.6. Raman spectra

The very weak photoluminescence of the films allows observing Raman scattering for *tBu*-$TAPH_2$, *tBu*-PcH_2, and *tBu*-NpH_2 as evident from Fig. 4. While the resonance Raman spectra of *tBu*-$TAPH_2$ (λ_{exc}: 543 nm) and *tBu*-PcH_2 (λ_{exc}: 542 and 633 nm) still show a broad luminescence background, that emission is suppressed with decreasing luminescence efficiency in the spectrum of *tBu*-NpH_2 (λ_{exc}: 633 nm). The tetraanthraporphyrazine AnH_2 does not show any Raman scattering irrespective of different excitation wavelengths used (λ_{exc}: 355, 543, 633, 806 nm). The resonance Raman spectra shown in Fig. 6 measured with higher resolution are subtracted by their fluorescence contribution.

The discussion of the assignment of the Raman bands will be reduced to some key features. To our knowledge Raman spectra of *tBu*-$TAPH_2$ have not yet been measured. This compound, however, representing the simplest structure of the porphyrazine system, should be a good model and should facilitate the assignments of the Raman bands in comparison with the spectra of the benzo-annelated porphyrazines.

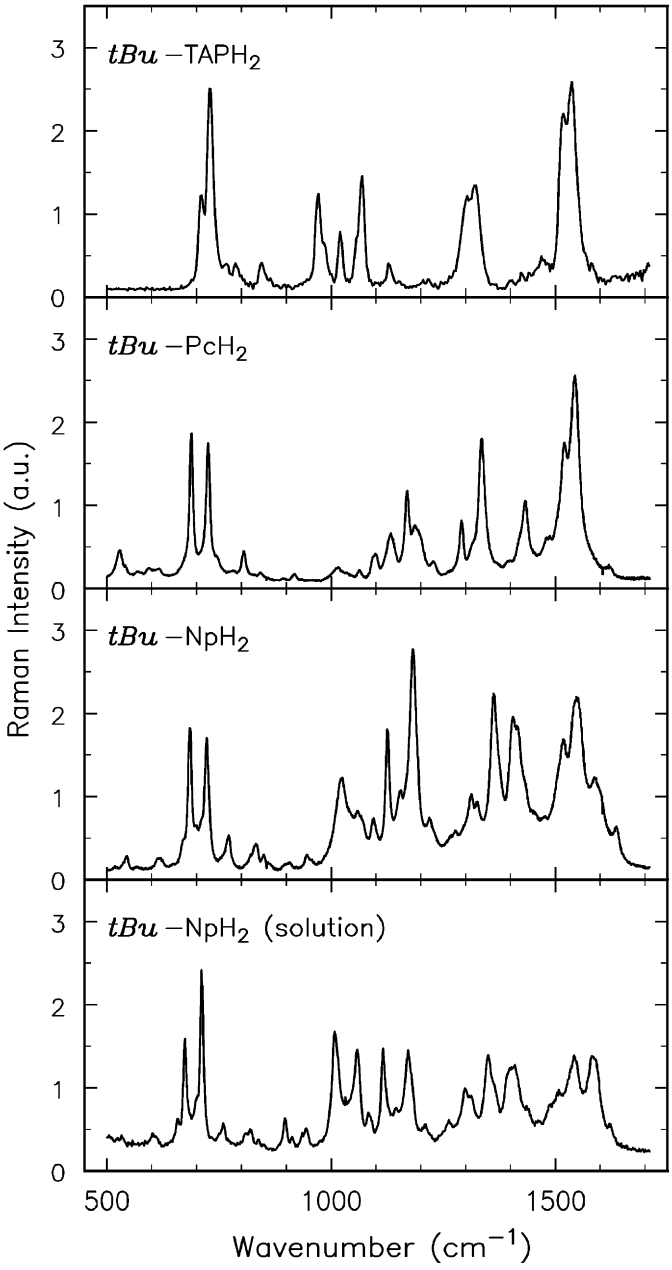

Fig. 6. High-resolution resonance Raman spectra for the films of *tBu*-$TAPH_2$, *tBu*-PcH_2, and *tBu*-NpH_2 films (excitation wavelengths as indicated in Fig. 4) as well as of a highly concentrated CCl_4 solution of *tBu*-NpH_2 ($c = 1.86 \times 10^{-2}$ M) illustrating a characteristic pattern for each porphyrazine.

We expect the resonance Raman spectrum of *tBu*-$TAPH_2$ in Fig. 6 to emerge from the characteristic vibrational modes of the core only. The appearance of the most intense Raman lines can be divided into four regions located at: (i) 1519 and 1538 cm^{-1}; (ii) 1305 and 1320 cm^{-1}; (iii) 972, 1020, and 1069 cm^{-1}; (iv) 710 and 730 cm^{-1}. From comparison with spectral position of Raman lines in pyrrole, isoindole, and porphyrine [65], it is very likely that the frequencies of the first group are

associated with coupled pyrrole C=C and aza C=N stretching vibrations. This assignment is also supported by normal mode analysis of unsubstituted copper phthalocyanine with D_{4h} symmetry, which indicates that all modes below 1700 cm^{-1} are strongly delocalized modes [66]. The modes between 1520 and 1550 cm^{-1} appear in all porphyrazines (Fig. 6).

Also the position of the modes in the range 690–730 cm^{-1} (Fig. 6) is very similar for the compounds. This group of modes can be associated with deformation and breathing vibrations of the macrocycle.

The vibrational modes in the region 1000–1500 cm^{-1}—probably also arising from coupling of pyrrole with the benzene moieties—clearly differ from those of the pattern of *tBu*-$TAPH_2$ reflecting the influence of the attached benzo groups. The bands above 1590 cm^{-1} in *tBu*-PcH_2 and *tBu*-NpH_2 can be attributed to the C–C stretches of benzene and naphthalene, respectively [24,25].

The different patterns of the Raman spectra for *tBu*-$TAPH_2$, *tBu*-PcH_2, and *tBu*-NpH_2 can be used as fingerprints to distinguish between the degrees of benzo-annelation in a porphyrazine system. It should be noted that small differences in the intensity of Raman lines of *tBu*-PcH_2 were observed using different excitation wavelengths at 543 and 633 nm, due to different vibronic coupling of the modes to the chromophor. This effect has also been noticed at PcH_2 [25] as well as in rare earth sandwich-type complexes of phthalocyanines [67]. The further the excitation wavelength is away from the absorption resonance, the more pronounced are the changes observed.

tBu-NpH_2 is the only compound which allows for observation of resonance Raman scattering in highly concentrated CCl_4 solution ($\sim 1.9 \times 10^{-2}$ M) (Figs. 3 and 6) due to formation of aggregates associated with efficient fluorescence quenching. Its Raman spectra in the film and in the aggregated form (solution) reveal some differences in the region of 1000–1500 cm^{-1}. Assuming that aggregates are a "precursor" of the solid state at the first glance, the differences in the spectral range might be associated with different intermolecular coupling and/or with a different orientation of the *tBu*Np-H_2 molecules. On the other hand, the difference in the band positions in the two spectra may also arise from changes in the relative intensities of the bands due to differences in relative resonance enhancement. This is most likely related to subtle symmetry changes between the molecules in film and in solution. Although aggregates of *tBu*-PcH_2 are also formed in concentrated CCl_4 solution ($\sim 9 \times 10^{-3}$ M) no Raman scattering was found at 633 or 543 nm excitation. *tBu*-$TAPH_2$ solutions do not show any indication of aggregation in CCl_4 even if the concentration is higher than 10^{-2} M.

4. Conclusions

For the first time a series of metal-free linearly benzo-annelated porphyrazines, tetra(*tert*-butyl) porphyrazine (*tBu*-$TAPH_2$), tetra(*tert*-butyl)phthalocyanine (*tBu*-PcH_2), tetra(*tert*-butyl)naphthalocyanine (*tBu*-NpH_2), and octaphenyltetraanthraporphyrazine (AnH_2), were studied in thin films by laser excitation at 543, 633, and 806 nm at room temperature using micro-Raman and luminescence spectroscopy. They reveal several interesting features which were not expected. For comparison the compounds were also studied in solution. With the exception of the smallest porphyrazine (*tBu*-$TAPH_2$) the absorption profiles of the thin films of *tBu*-PcH_2, *tBu*-NpH_2, and AnH_2 exhibit a strong broadening in comparison with the narrow Q-band in CCl_4 solution. This behaviour is explained by strong excitonic coupling. In the case of *tBu*-$TAPH_2$ the peripheral *tert*-butyl groups seem to prevent effective intermolecular coupling. In CCl_4 solution the long-wavelength absorption is strongly red-shifted by about 100 nm in going from *tBu*-$TAPH_2$, *tBu*-PcH_2, *tBu*-NpH_2, to AnH_2. In the films this bathochromic shift is of more complex nature. Moreover, the position of the absorption maxima for *tBu*-NpH_2 and AnH_2 films is additionally influenced by their thickness in contrast to *tBu*-$TAPH_2$ and *tBu*-PcH_2 films in the thickness range 100–500 nm. The luminescence is strongly quenched in the solid state and the maximum of the photoluminescence envelope exhibits a large Stokes shift which is associated with exciton coupling and a change of the conformation in the films. The Stokes shift of the fluorescence in CCl_4 amounts to a few nanometres only. Here it is shown and explained for the first time that films of two representatives—*tBu*-$TAPH_2$ and *tBu*-NpH_2—of the class of porphyrazines exhibit two luminescence bands with different Stokes shifts. This contrasts to *tBu*-PcH_2 films where only one luminescence band is observed.

In addition, the Raman signatures of *tert-butyl*- substituted porphyrazines were investigated. The differences in the Raman patterns of the compounds can be used to distinguish the degree of benzo-annelation. It is worth mentioning that also aggregates of *tBu*Np-H_2 representing a precursor of the solid state show resonance Raman modes similar to those of the film. No aggregation is found for *tBu*-TAP-H_2 even for concentrations higher than 10^{-2} M. This seems to be in accordance with the peculiarities of the absorption and photoluminescence spectra of this compound in the film.

To obtain a more detailed understanding of the strikingly different absorption and luminescence behaviour of the metal-free porphyrazine films, time-resolved measurements such as transient absorption spectroscopy are required. This is indispensable to understand the excited state properties more in detail of the films investigated.

Acknowledgements

The authors gratefully acknowledge the technical assistance of Katrin Herrmann and Katrein Bäurich.

References

[1] C.C. Leznoff, A.B.P. Lever (Eds.), Phthalocyanine, Properties and Applications, vol. 3, VCH, New York, 1989, pp. 170–225.
[2] T. Komori, Y. Amao, J. Porphyrins Phthalocyanines 6 (2002) 211.
[3] V. Aranyos, J. Hjelm, A. Hagfeldt, H. Grennberg, J. Porphyrins Phthalocyanines 5 (2001) 609.
[4] M.D.K. Nazeeruddin, R. Humphry-Baker, M. Grätzel, D. Wöhrle, G. Schnurpfeil, G. Schneider, A. Hirth, N. Trombach, J. Porphyrins Phthalocyanines 3 (1999) 230.
[5] D. Hohnholz, S. Steinbrecher, M. Hanack, J. Mol. Struct. 521 (2000) 231.
[6] Y. Qiu, Y. Gao, P. Wie, L.D. Wang, Appl. Phys. Lett. 80 (2002) 2628.
[7] F. Santerre, R. Cote, G. Veilleux, R.G. Saint-Jacques, J.P. Dodelet, J. Phys. Chem. 100 (1996) 7632.
[8] R.D. Gould, Coord. Chem. Rev. 156 (1996) 237.
[9] G. de la Torre, P. Vazquez, F. Agullo-Lopez, T. Torres, J. Mater. Chem. 8 (1998) 1671.
[10] B. Kessler, Appl. Phys. A 67 (1998) 125.
[11] L. Ottaviano, L. Lozzi, F. Ramondo, P. Picozzi, S. Santucci, J. Electron. Spectrosc. Relat. Phenom. 105 (1989) 148.
[12] I. Biswas, H. Peisert, T. Schwieger, D. Dini, M. Hanack, M. Knupfer, T. Schmidt, T. Chasse, J. Chem. Phys 122 (2005) 064710/1.
[13] D. Pop, B. Winter, W. Freyer, I.V. Hertel, W. Widdra, J. Phys. Chem. B 107 (2003) 11643.
[14] W. Freyer, S. Mueller, K. Teuchner, J. Photochem. Photobiol. A: Chemistry 163 (2004) 231.
[15] A.C. de Wilton, L.V. Haley, J.A. Königstein, J. Phys. Chem. 88 (1984) 1077.
[16] Y. Sakakibara, R.N. Bera, T. Mizutani, K. Ishida, M. Tokumoto, T. Tani, J. Phys. Chem. B 105 (2001) 1547.
[17] K. Yoshino, M. Hikida, K. Kaneto, Y. Inushi, Technol. Rep. Osaka Univ. 23 (22005) (1973) 171.
[18] S.M. Bayliss, S. Heutz, G. Rumbles, T.S. Jones, Phys. Chem. Chem. Phys. 1 (1999) 3673.
[19] E.R. Menzel, K.J. Jordan, Chem. Phys. 32 (1978) 223.
[20] G.L. Pakhomov, D.M. Gapanova, A.Y. Luk'yanov, E.S. Leonov, Phys. Solid State 47 (2005) 170.
[21] K. Yoshino, M. Hikida, K. Tatsuno, K. Kaneto, Y. Inushi, J. Phys. Soc. Jpn 34 (1973) 441.
[22] B. Blanzat, C. Barthou, N. Tercier, J. Am. Chem. Soc. 109 (1987) 6193.
[23] G. Blasse, G.J. Dirksen, A. Maijerink, J.F. van der Pol, E. Neeleman, W. Drenth, Chem. Phys. Lett. 154 (1989) 421.
[24] R. Aroca, D.P. Dilella, R.O. Loutfy, J. Phys. Chem. Solids 43 (1982) 707.
[25] I. Gobernado-Mitre, R. Aroca, Chem. Mater. 7 (1995) 118.
[26] N. Kobayashi, S. Nakajima, H. Ogata, T. Fukuda, Chem. Eur. J. 10 (2004) 6294.
[27] P.S. Vincett, Z.D. Popovic, L. McIntyre, Thin Solid Films 82 (1981) 357.
[28] S.M. Bayliss, S. Heutz, R. Cloots, R.L. Middleton, G. Rumbles, T.S. Jones, Adv. Mater. 12 (2000) 202.
[29] T. Saji, Chem. Lett. 4 (1988) 693.
[30] Y. Harima, K. Yamashita, J. Phys. Chem. 93 (1989) 4184.
[31] W. Freyer, L.Q. Minh, Monatsh. Chem. 117 (1986) 475.
[32] N. Kobayashi, S. Nakajima, T. Osa, Inorgan. Chim. Acta 210 (1993) 131.
[33] J. Mizuguchi, S. Matsumoto, J. Phys. Chem. 103 (1999) 614.
[34] M. Gouterman, C. Weiss, H. Kobayashi, J. Mol. Spectrosc. 16 (1965) 415.
[35] M. Kasha, H.R. Rawls, M.A. El-Bayoumi, Pure Appl. Chem. 11 (1965) 371.
[36] A.S. Davydov, Theory of Molecular Excitons, McGraw-Hill, New York, 1962.
[37] J.A. Tant, Y.H. Geerts, M. Lehmann, V. De Cupere, G. Zucchi, B.W. Laursen, T. Bjornholm, V. Lemaur, V. Marcq, A. Burquel, E. Hennebicq, F. Gardebien, P. Viville, D. Beljonne, R. Lazzaroni, J. Cornil, J. Phys. Chem. B 109 (2005) 20315.
[38] W.J. Pietro, T.J. Marks, M.A. Ratner, J. Am. Chem. Soc. 107 (1985) 5837.
[39] P. Devaux, Mol. Phys. 23 (1972) 265.
[40] L.E. Lyons, J.R. Walsh, J.W. White, J. Chem. Soc. (1960) 167.
[41] E.A. Lucia, F.D. Verderame, J. Chem. Phys. 48 (1968) 2674.
[42] H. Yanagy, T. Kouzeki, M. Ashida, T. Noguchi, J. Appl. Phys. 71 (1992) 5146.
[43] N.M. Amar, R.D. Gould, A.M. Saleh, Curr. Appl. Phys. 2 (2002) 455.
[44] H. Peisert, T. Schwieger, J.M. Auerhammer, M. Knupfer, M.S. Golden, J. Fink, P.R. Bressler, M. Mast, Chem. Phys. Lett. 90 (2001) 466.
[45] S. Heutz, S.M. Bayliss, R.L. Middelton, G. Rumbless, T.S. Jones, Phys. Chem. B 104 (2000) 7124.
[46] S. Dhami, A.J. de Mello, G. Rumbles, S.M. Bishop, D. Phillips, A. Beeby, Photochem. Photobiol. 61 (1995) 341.
[47] P.P. Pompa, G. Ciccarella, J. Spadavecchia, R. Cingolani, G. Vasapollo, R. Rinaldi, J. Photochem. Photobiol. A: Chemistry 163 (2004) 113.
[48] T. Gunaratne, V.O. Kennedy, M.E. Kenney, M.A.J. Rodgers, J. Phys. Chem. 108 (2004) 2576.
[49] L. Oddos-Marcel, F. Madeore, A. Bock, D. Neher, A. Ferencz, H. Rengel, G. Wegner, C. Kryschi, H.P. Trommsdorff, J. Phys. Chem. 100 (1996) 11850.
[50] M. Fujitsuka, O. Ito, H. Konami, Bull. Chem. Soc. Jpn 74 (2001) 1823.
[51] A.V. Nikolaitchik, O. Korth, M.A.J. Rogers, J. Phys. Chem. A 103 (1999) 7587.
[52] T. Nakanishi, K. Mizi, A. Matsui, H. Nishimura, J. Lumin. 47 (1991) 303.
[53] P. Schouwink, G. Gadret, R.F. Mahrt, Chem. Phys. Lett. 341 (2001) 213.
[54] H. Langhals, O. Krotz, K. Polborn, P. Mayer, Angew. Chem. 117 (2005) 2479.
[55] I. Wang, E. Botzung-Appert, O. Stephan, A. Ibanez, P.L. Baldeck, J. Opt. A: Pure Appl. Opt. 4 (2002) S258.
[56] D. Weiss, R. Kietzmann, J. Mahrt, B. Tufts, W. Storck, F. Willig, J. Phys. Chem. 96 (1992) 5320.
[57] A. Nollau, M. Hoffmann, T. Fritz, K. Leo, Thin Solid Films 368 (2000) 130.
[58] K. Puech, H. Fröb, M. Hoffman, K. Leo, Opt. Lett. 21 (1996) 1606.
[59] B. Stevens, Spectrochim. Acta 18 (1962) 439.
[60] I. Akimoto, K. Kan'no, H. Osuga, K. Tanaka, J. Lumin. 112 (2005) 341.
[61] C.J. Tonzola, M.M. Alam, S.A. Jenekhe, Adv. Mater. 14 (2002) 1806.
[62] V.N. Bliznyuk, S.A. Carter, J.C. Scott, G. Klärner, R.D. Miller, D.C. Miller, Macromolecules 32 (1999) 361.
[63] G.E. Johnson, J. Chem. Phys. 61 (1974) 3002.
[64] E. Orti, J.L. Bredas, C. Clarisse, J. Chem. Phys. 92 (1990) 1228.
[65] P. Stein, J.M. Burke, T.G. Spiro, J. Am. Chem. Soc. 97 (1975) 2304.
[66] R. Aroca, Z.Q. Zeng, J. Mink, Phys. Chem. Solids 51 (1990) 135.
[67] J. Jiang, U. Cornelissen, D.P. Arnold, X. Sun, H. Homborg, Polyhedron 20 (2001) 557.